



20 m Annual Paddy Rice Map for Mainland Southeast Asia Using Sentinel-1 SAR Data

Chunling Sun^{1,2,3}, Hong Zhang^{1,2,3*}, Lu Xu^{1,2}, Ji Ge^{1,2,3}, Jingling Jiang^{1,2,3}, Lijun Zuo^{1,2}, Chao Wang^{1,2,3}

¹Key Laboratory of Digital Earth Science, Aerospace Information Research Institute, Chinese Academy of Sciences, Beijing 100094, China

²International Research Center of Big Data for Sustainable Development Goals, Beijing 100094, China

³College of Resources and Environment, University of Chinese Academy of Sciences, Beijing 100049, China

Correspondence to: Hong Zhang (zhanghong@radi.ac.cn)

10 **Abstract.** Over 90% of the world's rice is produced in the Asia-Pacific Region. Synthetic aperture radar (SAR) enables all-day and all-weather observations of rice distribution in tropical and subtropical regions. Rice growth patterns in tropical and subtropical regions are complex, and it is difficult to construct representative rice growth patterns, which makes it much more difficult to extract rice distribution based on SAR data. To address this problem, a rice mapping method based on time-series Sentinel-1 SAR data is proposed in this study for large regional tropical or subtropical areas. Based on the analysis of rice
15 backscattering characteristics in mainland Southeast Asia, the combination of spatio-temporal statistical features with the generalization ability to complex rice growth patterns was selected, then input into the U-Net semantic segmentation model and combined with WorldCover data to eliminate false alarms, and finally the 20-meter resolution rice map of five countries in mainland Southeast Asia in 2019 was obtained. On the validation sample set, the proposed method achieved an accuracy of 92.20%. Good agreement was obtained when comparing our rice map with statistical data and other rice maps at the national
20 and provincial levels. The maximum coefficient of determination R^2 was 0.93 at the national level and 0.97 at the provincial level. These results demonstrate the advantages of the proposed method in rice extraction with complex cropping patterns and the reliability of the generated rice maps. The 20 m annual paddy rice map for mainland Southeast Asia is available at <https://doi.org/10.5281/zenodo.7315076>(Sun, 2022).

1 Introduction

25 Among the 17 sustainable development goals (SDGs) set by the United Nations in 2015, eradicating hunger, achieving food security and improving nutrition, and promoting sustainable agriculture are key components of Goal 2 "Zero Hunger"(Desa, 2016). Rice feeds more than half of the world's population as a staple food and is a major crop for world food security (Kuenzer and Knauer, 2012). Asia is the largest rice-producing region in the world (Chen et al., 2012). With 48 million hectares under rice cultivation, Southeast Asia accounts for 40% of global rice exports(Yuan et al., 2022). The dual pressure of population
30 and environment threatens the sustainability of global food security(Faostat, 2010; Godfray et al., 2010). Accurate information



on planted area and spatial distribution is the basis for monitoring rice growth and predicting yield (Mosleh et al., 2015; Laborte et al., 2017; Clauss et al., 2018; Jin et al., 2018; Yu et al., 2020; Hoang-Phi et al., 2021).

Remote sensing technology plays a crucial role in rice growth monitoring and distribution mapping (Weiss et al., 2020; Zhao et al., 2021; Tsokas et al., 2022). Rice area mapping at the national scale usually uses medium- and low-resolution optical remote sensing data, such as MODIS and Landsat data. Some researchers used MODIS multitemporal data to produce rice maps of China with resolutions of 500 m, 250 m and 500 m respectively (Sun et al., 2009; Clauss et al., 2016; Qiu et al., 2022). Guan et al. produced rice maps of Vietnam at 500 m resolution using MODIS time series data in 2010 (Guan et al., 2016). The National Agricultural Statistics Service (NASS) released the state-based Crop Data Layer (CDL), a 30-m resolution crop distribution map product for the entire continental United States, using multisource medium resolution remote sensing data (Landsat, IRS-p6, DEIMOS-1, etc.) (Johnson and Mueller, 2010). Luo et al. and Wei et al. used Landsat time-series data to produce 1 km and 30 m resolution rice datasets for China, respectively (Luo et al., 2020a; Luo et al., 2020b; Wei et al., 2022). Recently, the Sentinel-2 satellite sensor opens up new possibilities for paddy rice monitoring. Liu et al. obtained medium-resolution rice maps of China using Sentinel-2 time series data in 2020 (Liu et al., 2022).

At the continental scale, MODIS time-series data were frequently used to map the distribution of rice cultivation (Dong et al., 2016a; Dong et al., 2016b). Xiao et al. and Gumma et al. produced low- and medium-resolution rice area maps for several South and Southeast Asian countries using MODIS data at the 500 m spatial resolution, respectively (Xiao et al., 2005; Xiao et al., 2006; Gumma et al., 2011a; Gumma et al., 2011b; Bridhikitti and Overcamp, 2012; Gumma et al., 2014; Nelson and Gumma, 2015). Using MODIS time-series data, Zhang et al. generated rice acreage maps for China and India from 2000 to 2015 (Zhang et al., 2017). Han et al. used MODIS data to complete 500 m annual rice maps for the Asian monsoon region from 2000 to 2020 (Han et al., 2022). SPOT data were also used for continent-wide rice mapping. Manjunath et al. used 2009-2010 multi-temporal SPOT VGT normalized difference vegetation index (NDVI) data to produce 1 km resolution rice maps for South and Southeast Asia (Manjunath et al., 2015).

Most of the rice in the world is distributed in hot and rainy areas. However, optical data are easily obscured by clouds, which also poses a challenge for rice extraction in humid and sub-humid climates with abundant water resources such as Southeast Asia (Zhu and Woodcock, 2012; Liu et al., 2019; Sun et al., 2021). Compared with traditional optical remote sensing, synthetic aperture radar (SAR) is an active microwave radar with the advantages of all-day and all-weather, which is weather-independent and can penetrate clouds, and is very sensitive to the geometric structure and dielectric properties of crops (Huang et al., 2017; Orynbaikyzy et al., 2019; Sun et al., 2022). In recent years, free SAR data represented by Sentinel-1 data have been widely used in rice mapping over large regions. Singha et al. obtained seasonal rice maps at 10 m resolution for Bangladesh and northeast India using time-series Sentinel-1VH data for 2017 (Singha et al., 2019). Pan et al. used 2016-2020 Sentinel-1VH data to produce 10-m spatial resolution double-season rice maps for nine provinces in southern China (Pan et al., 2021). Xu et al. used time-series Sentinel-1VH data to obtain a 20 m rice map for Thailand in 2019 (Xu et al., 2021).

To take full advantage of multi-source remote sensing data, some researchers combined optical and SAR time-series data in the large-scale rice mapping studies (Thenkabail et al., 2009; Zhang et al., 2018; You and Dong, 2020). Phan et al. used



65 Sentinel 1/2 and Landsat data to produce the first Vietnam land use/land cover annual dataset with 30m resolution from 1990 to 2020 (Phan et al., 2021). Han et al. obtained 500m resolution rice maps from 2017 to 2019 in Northeast and Southeast Asia using Sentinel-1 and MODIS time-series data (Han et al., 2021).

At present, large-scale rice mapping methods based on remote sensing data can be divided into two categories, one is the combination of phenological information and remote sensing images, and the other is the combination of time series data and machine learning relying on image information. The phenology-based approach refers to the extraction of rice by defining phenological indicators or identifying phenological periods by combining the time-series data of the rice growth cycle and the analysis of the growth phenology calendar (Nelson et al., 2014; Chen et al., 2016; Nguyen and Wagner, 2017; Liu et al., 2018; Xin et al., 2020; Ni et al., 2021). The phenological periods such as transplanting, flooding, heading and maturity are most often used to extract rice. Shew et al. combined vegetation indices extracted from Landsat time-series data with a rule-based algorithm for phenological stages to map a 30 m dry season rice map of Bangladesh from 2014 to 2018 (Shew and Ghosh, 2019). Li et al. extracted the minimum and maximum values of permanent water backscatter coefficients and three thresholds of phenological characteristics, namely, the date of the beginning of the season, date of maximum backscatter during the peak growing season, and length of the vegetative stage from 402 scenes of Sentinel-1 data in 2017 to map rice paddies in the Mun River basin, Thailand (Li et al., 2020). Kang et al. completed a 10 m resolution rice map of Cambodia from Sentinel-1 (2015) and Sentinel-2 (2015-2017) time-series data using three key rice phenological periods in the dry and rainy seasons, respectively (Kang et al., 2022).

However, the phenology-based methods rely too much on human intervention and are not suitable for rice extraction with complex cropping cycles. The approaches based on the combination of time series data and machine learning method refer to the direct use of time series as the input features for machine learning (Ndikumana et al., 2018; Chang et al., 2020; Mansaray et al., 2021; Yang et al., 2021). Machine learning methods are used to extract rice information by mining fixed relationships across growth periods of rice (Yang et al., 2019; You et al., 2021). Torbick et al. used Sentinel-1, Landsat-8 and PALSAR-2 time series data and a random forest algorithm to map rice planting area and planting intensity of Myanmar with 20 m resolution in 2015 (Torbick et al., 2017). Inoue et al. developed a 30 m resolution map of paddy rice in Japan for 2018 using Sentinel-1 SAR data and Sentinel-2 data with the conventional decision tree methods (Inoue et al., 2020). Wei et al. completed rice area mapping for the Arkansas River Basin, USA, by entering dual-polarized Sentinel-1 data from 2017-2019 into a modified U-Net model (Wei et al., 2021). Soh et al. used Sentinel-1 and Sentinel-2 time series data and a K-means clustering method to map rice in West Malaysia (Soh et al., 2022).

The climate in tropical or subtropical regions such as Southeast Asia is suitable for rice growth throughout the year, increasing the difficulty of rice extraction. First, it is difficult to obtain accurate phenological information because the climate in Southeast Asia is hot and humid for rice growth, the timing of rice seedling and transplanting is more flexible (Xu et al., 2021). This makes it impossible to use empirical methods to determine effective weathering indicators and suitable periods. Second, rice growth patterns in Southeast Asia are too complex to construct a representative rice growth model (Kang et al., 2022). This poses obstacles for rice extraction methods that utilize time-fixed relationships in time-series data.



100 Current publicly downloadable rice products for Southeast Asia include the Asia rice map (IRRI Rice Data, 500 m) (Nelson and Gumma, 2015), Vietnam-wide annual land use/land cover datasets from 1990 to 2020 (VLUCD, 30 m) (Phan et al., 2021), annual paddy rice maps for Northeast and Southeast Asia from 2017 to 2019 (NESEA-Rice10, 10 m) (Han et al., 2021), and annual rice in the Asian monsoon region from 2000 to 2020 (500 m) (Han et al., 2022). Except for Vietnam's VLUCD, the source data for the public rice maps in Southeast Asia were mainly MODIS. Rice maps using MODIS data contained a large number of mixed pixels due to low spatial resolution (Dong et al., 2015; Shew and Ghosh, 2019), which affected the accuracy of rice maps.

Therefore, in this study, to meet the requirements of high-precision rice area mapping in Southeast Asia, the objectives accomplished using Sentinel-1 time-series data are as follows.

- 110 (1) A new feature extraction method is proposed by analyzing the time-series backscattering variation of rice in mainland Southeast Asia. The method does not need to summarize the general evolutionary model from rice backscatter coefficients with diverse growth patterns. Using three simple but effective temporal statistical features defined in this study, it is possible to capture features that provide key information about the rice growth process. This study provided a new idea for rice mapping methods in tropical or subtropical regions.
- 115 (2) A deep combination of the above features and the U-Net model will be used to fully exploit the pixel-level semantic features to complete the annual rice mapping of five Southeast Asian countries in 2019, enriching the available Southeast Asian rice maps, and providing support information for the scientific community and scientific decision-making.

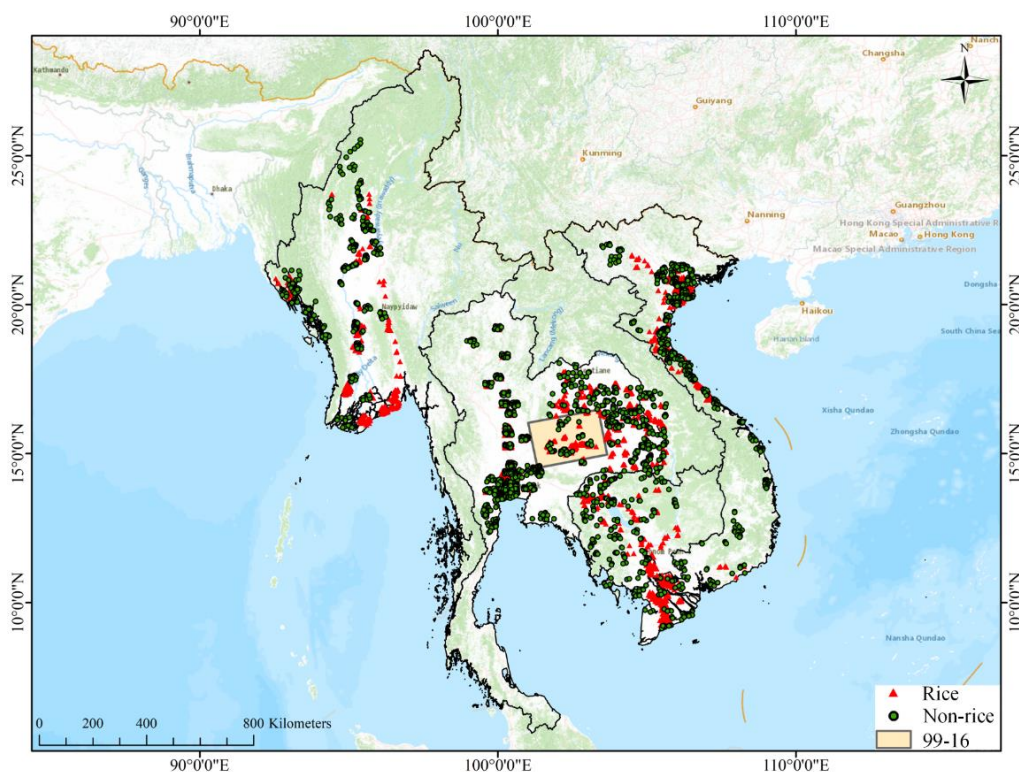
The rest of the paper is organized as follows. Section 2 describes the study area and the data information used; Section 3 presents the rice mapping scheme; Section 4 presents the temporal characteristics analysis of the data and the rice map results; Section 5 discusses the results; and finally, Section 6 draws conclusions.

2 Materials

120 2.1 Study area

Approximately 90% of the world's rice is grown on 140 million hectares of land in Asia. The rice production in mainland Southeast Asian accounts for about 15% of the world rice production (Fao, 2020).. The study area is five countries in mainland Southeast Asia, namely, Myanmar, Thailand, Laos, Cambodia, and Vietnam, as shown in Figure 1. These countries have more land under rice cultivation than any other crop. And Vietnam and Thailand are the two largest rice exporters in the world (Yuan et al., 2022). Indeed, changes in rice production in these countries could destabilize international rice markets and have a clear impact on global food security.

Southeast Asia has a tropical monsoon climate with an average annual temperature of 20-27 °C and abundant rainfall. Therefore, rice can be grown at any time of the year. Agricultural systems in Southeast Asia are dominated by rainfed lowland rice and irrigated lowland rice (Kuenzer and Knauer, 2012). Under suitable irrigation conditions, rice can be harvested two to 130 three times per year.



135 **Figure 1: Location of the study area. Orbit-frame 99-16 images are used for the training samples, and the Rice and Non-rice flags show the distribution of the validation sample set. The base map is from Esri.**

2.2 Data source

2.2.1 Satellite imagery and auxiliary data

The European Space Agency (ESA) provides a free data source for large-scale land cover monitoring through Sentinel-1A, launched in 2014, and Sentinel-1B, launched in 2016 (Torres et al., 2012). The Sentinel-1 satellites carry a C-band (5.405 GHz) synthetic-aperture radar with a 12-day revisit period. In this study, the 2019 dual-polarized (VV/VH) GRD products in Interferometric Wide Swath (IW) mode were downloaded from the ASF website. In total, 12 tracks, 90 frames and 2665 scenes of data were acquired. Details are shown in Table 1.

And, the DEM and land use/land cover product were also collected. Shuttle Radar Topography Mission (SRTM) 3sec DEM product was used for terrain correction of SAR data. WorldCover data were used to reduce false alarms caused by water and woodland. WorldCover is a global land cover product produced by ESA and several scientific institutions using Sentinel-1 and -2 data (Zanaga et al., 2021). It provides information on 11 land cover types for 2020 with a resolution of 10 m and an overall accuracy of 80.7% for the Asian region.



Table 1 List of SAR data

Country	Orbit	Frame	Satellite	Number of images	Country	Orbit	Frame	Satellite	Number of images
Experimental Data									
Thailand	172	17	S1A	31	Laos	99	1240	S1A	30
		18	S1A	31			1245	S1A	30
	135	16	S1A	23			1250	S1A	30
		17	S1A	23		26	44	S1A	31
		18	S1A	23			49	S1A	31
	19	S1A	23	54			S1A	31	
	62	1	S1B	29			59	S1A	31
		2	S1B	29			64	S1A	31
		3	S1B	29		69	S1A	31	
		4	S1B	29		128	44	S1A	30
		5	S1B	29			49	S1A	30
		20	S1A	27			54	S1A	30
		21	S1A	27	59		S1A	30	
		22	S1A	26	64	S1A	30		
	23	S1A	24	Myanmar	41	44	S1A	31	
	24	S1A	25			50	S1A	31	
	164	1	S1B			32	55	S1A	31
		2	S1B			32	60	S1A	31
		3	S1B			32	65	S1A	31
		4	S1B		32	70	S1A	31	
		5	S1B		32	143	46	S1A	30
		20	S1A		13		51	S1A	30
	91	1	S1B		32		56	S1A	30
		2	S1B		32		61	S1A	30
3		S1B	32		66		S1A	30	
4		S1B	32		71		S1A	30	
Cambodia	99	1220	S1A	30	76		S1A	30	
		1225	S1A	30	70	1217	S1A	31	
		31	S1B	31		1222	S1A	31	
	26	29	S1A	28		1227	S1A	31	
		32	S1B	30		1232	S1A	31	
		38	S1B	30		1237	S1A	31	
128	43	S1B	30	1242		S1A	31		
	34	S1A	30	1247		S1A	31		
	39	S1A	30	1252		S1A	31		
Vietnam	26	23	S1A	28		1257	S1A	31	
		34	S1A	31		1262	S1A	31	
	55	31	S1A	31	1267	S1A	31		
		37	S1A	31	172	1248	S1A	28	
		42	S1A	31		1253	S1A	28	
		47	S1A	31		1258	S1A	28	
		62	S1A	31		1263	S1A	28	
		67	S1A	31		1268	S1A	28	
	72	S1A	31	1273		S1A	28		
	128	29	S1A	30					
69		S1A	30						
Training data set									
Thailand	99	16	S1A	29					



2.2.2 Agricultural statistics

150 The statistical yearbooks of each country were collected to compile annual census data of rice harvested area at different administrative levels in these countries. The administrative levels include national and subnational levels (state, province, or regions, uniformly represented by province in this study). The unit of area in the statistical data is uniformly converted to hectares (ha).

2.2.3 Available rice maps based on remote sensing data

155 From the perspective of resolution and coverage area, 2 publicly downloadable rice maps were selected for comparison.

(1) Vietnam-wide annual land use/land cover datasets (VLUCD)

160 Researchers from the Japan Aerospace Exploration Agency (JAXA) produced the first 30-m resolution Vietnam-wide annual land use/land cover datasets (VLUCD) using multiple sources of data (including Landsat and Sentinel-1/2) and a random forest algorithm (Phan et al., 2021). The VLUCD contains annual land cover products for 1990-2020, including a primary classification (containing 10 different categories of primary land cover, including rice) and a secondary classification (18 different categories of secondary primary land cover, including rice). The rice layer was extracted from the 2019 annual land cover products for comparison.

(2) Rice data of Asia from International Rice Research Institute (IRRI Rice Data)

165 The International Rice Research Institute (IRRI) is an international agricultural research and training organization with its headquarters in Los Baños, Laguna, in the Philippines, and offices in seventeen countries. IRRI is one of 15 agricultural research centers in the world that form the Consortium of International Agricultural Research Centers (CGIAR), a global partnership of organizations engaged in research on food security. IRRI is also the largest non-profit agricultural research center in Asia.

170 The IRRI produced a 500 m resolution map of the general distribution of rice in Asia from 2001 to 2012 using MODIS time-series data (Nelson and Gumma, 2015), which is freely available to the public.

Table 2 shows details of the SAR data, auxiliary data, available rice maps, land cover data and statistics used in the study.

Table 2 Details of the data used in the study

Data type	Data product or country name	Year	Resolution	Description	Data access	Last access (dd/mm/yyyy)
SAR imagery	Sentinel-1	2019	20*22 m (rg*az)	The backscatter characteristics extraction	https://search.asf.alaska.edu/#/	11/10/2022
DEM	Shuttle Radar Topography	2000	90m	Terrain correction	https://search.earthdata.nasa.gov/search?q=SRTM	11/10/2022



	Mission (SRTM) 3sec					
Land cover data	ESA WorldCover 2020	2020	10 m	Extraction of water and forest mask	https://esa-worldcover.org/en	11/10/2022
Available Rice Map	Vietnam-wide annual land use/land cover datasets (VLUCD)	2019	30 m	Spatial consistency comparison of rice extraction results	https://www.eorc.jaxa.jp/ALOS/en/dataset/lulc/lulc_vnm_v2109_e.htm	11/10/2022
	Rice data of Asia from IRRI (IRRI Rice Data)	2000 to 2012	500 m	Spatial consistency comparison of rice extraction results	https://www.irri.org/mapping	11/10/2022
Statistical yearbook	Vietnam	2019	Province scale	verifying the classification accuracy	https://www.gso.gov.vn/en/homepage/	11/10/2022
	Cambodia	2019	Province scale	verifying the classification accuracy	http://nis.gov.kh/index.php/km/	11/10/2022
	Laos	2019	Province scale	verifying the classification accuracy	https://www.lsb.gov.la/en/home/	11/10/2022
	Thailand	2019	Province scale	verifying the classification accuracy	http://www.nso.go.th/sites/2014en	11/10/2022
	Myanmar	2019	State scale	verifying the classification accuracy	https://www.mopf.gov.mm/en/page/planning/central-statistical-organization-cso/752	11/10/2022

3 Method

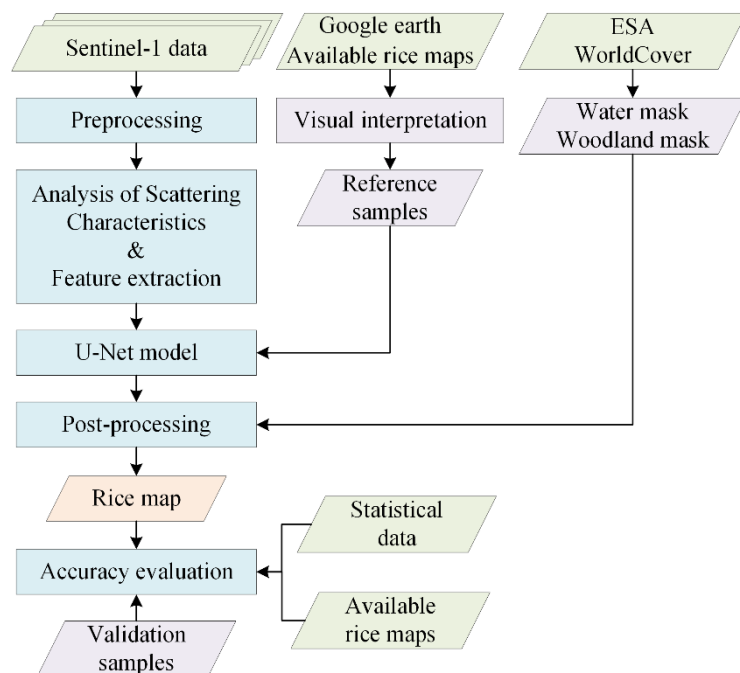
175 The flowchart of this study is shown in Figure 2. First, the Sentinel-1 time series images were preprocessed. Then, key features in the rice growth process are extracted from the time series SAR data. To make full use of the pixel-level semantics of the features, the extracted features were fed into the U-Net model to obtain rice extraction results with spatial details. Finally, to reduce false alarms from water bodies and vegetation, the results were postprocessed using masks generated based on high-precision land cover products to obtain the annual rice map of five Southeast Asian countries.

180 3.1 Preprocessing

The Sentinel-1 time-series data were preprocessed using SNAP software (Filipponi, 2019). The steps were as follows: (1) orbit correction; (2) thermal noise removal; (3) radiometric calibration; (4) coregistration; (5) terrain correction; (6) multitemporal



speckle noise filtering; and (7) conversion of the multitemporal intensity map to sigma 0 (σ^0) on the decibel (dB) scale. The final σ^0 images with 20 m resolution in the WGS84 geographic coordinate system were obtained.



185

Figure 2: Flowchart of the proposed rice mapping method using Sentinel-1 data.

3.2 Feature Extraction

As described in many previous studies (Singha et al., 2019; Chang et al., 2020; Crisóstomo De Castro Filho et al., 2020; Sun et al., 2022), VH polarization was more sensitive to the flooding period of rice than VV polarization and has been more widely used for rice extraction. Therefore, VH data were selected in this study. To analyze the time-series characteristics of the backscattering coefficients of rice and other land cover types in the study area, representative sample plots of four typical land cover types (rice, water bodies, buildings, and vegetation) were selected. Based on Google Earth data and other land cover data, four rice regions that belongs to different cropping systems were chosen. The average VH polarization time series data of these land cover types were calculated, as shown in Figure 3.

190

195

In Figure 3, the backscattering coefficients of water bodies were small, as they exhibited single specular scattering, and their return power level was lower than other land covers. In contrast, buildings exhibited double bounce and their return powers were much stronger, leading to larger backscattering coefficients. The scattering process of radar waves of vegetation was more complicated, and the backscattering coefficients of vegetation were between buildings and water bodies. For different kinds of rice samples, the curve fluctuations were significant, due to the effects of flooding and the multi-season planting patterns. But generally, their backscattering intensities ranged between buildings and water bodies. More specifically, the land parcel of Rice 1 was planted with two seasons of rice during the observation period: the first season was from April to July,

200



and the second season was from August to October. The land parcel of Rice 2 was planted with only one season of rice, from April to September. The land parcel of Rice 3 was planted with two seasons of rice: the first season was from March to July and the second season was from July to October. The land parcel of Rice 4 was planted with three seasons of rice: the first season was from February to June, the second season was from June to October, and only part of the third season (October-December) was observed. It can be seen that the time steps of each growing season for the selected Rice 1- Rice 4 were inconsistent. In fact, the high heterogeneity of rice backscattering coefficients in Southeast Asia is caused by the high heterogeneity in climate and topography. This makes the backscatter coefficient curves of the rice growth cycle more diverse and does not allow us to summarize a generalized model of rice evolution. Therefore, it will be difficult to accomplish the rice extraction task using a direct reliance on the fixed relationship between phenology and time.

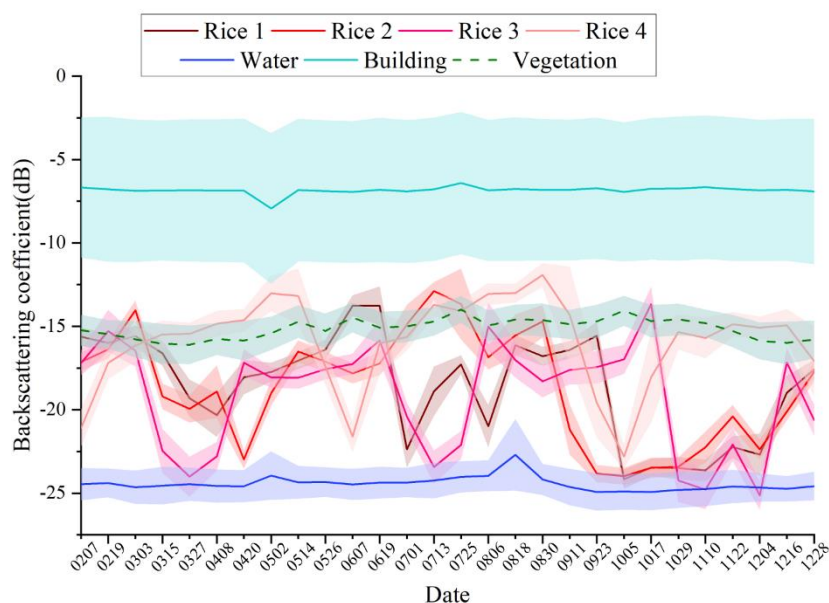


Figure 3: The average VH polarization backscattering coefficient curve of typical landcovers

Through a large number of comparative experimental analysis and combined with our previous research work (Xu et al., 2022), three time-series statistical features that can describe the most significant SAR characteristics during rice growth were selected for rice mapping in the study area, namely, the sharpness of the change in σ^0 (σ_{var}^0), the minimum value of the backscatter coefficients in the time-series (σ_{min}^0), the maximum value of backscatter coefficients in the time-series (σ_{max}^0).

The interaction between the crop canopy and microwave radiation varies with time during plant growth. In contrast, the backscattering coefficients of non-crops, such as water bodies, buildings and forest, are more stable. Therefore, the sharpness of the change in σ^0 with time will be a key factor in distinguishing cropland from other land cover types. σ_{var}^0 is given by the following equation.



$$\sigma_{var}^0 = \frac{1}{n} \sum_i^n |\sigma_i^0 - \sigma_{mean}^0|^2 \quad (1)$$

where $\sigma_{mean}^0 = \frac{1}{n} \sum_i^n \sigma_i^0$, n is the number of images.

The presence of a flooding period makes rice differ significantly from other crops in terms of backscattering characteristics. The backscattering coefficient of rice in the flooding period is close to that of the water body. Therefore, this study identified the flooding period by calculating the minimum value of the backscatter coefficient in the time-series images to distinguish rice from other crops. σ_{min}^0 is given by Equation (2).

$$\sigma_{min}^0 = \min\{\sigma_1^0, \sigma_2^0, \sigma_3^0, \dots, \sigma_n^0\} \quad (2)$$

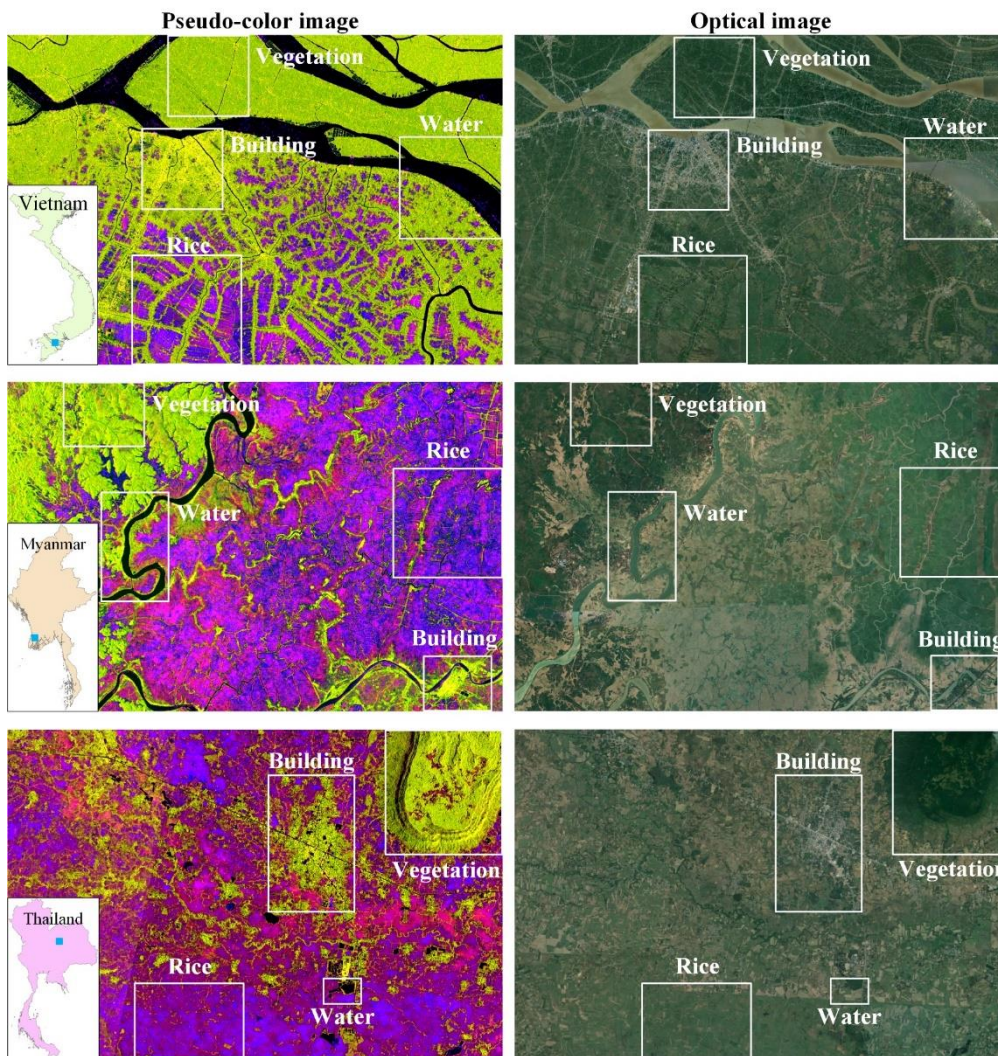


Figure 4: The Pseudo-color image of typical land cover types in different countries (R: σ_{max}^0 ; G: σ_{min}^0 ; B: σ_{var}^0 ;Optical images are from Google Earth ©Google Earth).



230 The seasonal backscattering variation exhibited by water bodies can interfere with the identification of rice. In contrast to the seasonal variation of water bodies, the backscatter coefficient of rice shows a substantial increase during the growth process. Therefore, false alarms generated by water bodies can be reduced by identifying the maximum value of backscatter coefficients in the time-series images. σ_{max}^0 is given by the following equation.

$$\sigma_{max}^0 = \max\{\sigma_1^0, \sigma_2^0, \sigma_3^0, \dots, \sigma_n^0\} \quad (3)$$

A pseudo-color image is synthesized in the order of R: σ_{max}^0 , G: σ_{min}^0 , and B: σ_{var}^0 . False color images of typical land cover for several countries and the corresponding optical images in Google Earth are given in Figure 4. Due to the higher σ_{var}^0 and σ_{max}^0 and lower σ_{min}^0 of rice, the color of rice in the pseudo-color composite image is mainly purplish red, sometimes red or dark blue. Compared to other land covers, water bodies have lower σ_{var}^0 , σ_{max}^0 and σ_{min}^0 . Therefore, water bodies are black in the false color composite. Land covers with less variation in backscatter intensity, such as buildings and vegetation, generally have smaller σ_{var}^0 and higher σ_{min}^0 . Therefore, the colors of these land covers are usually yellow or green in the pseudo-color image.

3.3 Training and validation sets

The above analysis shows that, the rice and non-rice landcovers of these Southeast Asian countries have consistent features in the pseudo-color image, which means that the model trained by one scene was applicable for all other scenes. Therefore, a training dataset generated from the orbit-frame 99-16 images of Thailand from previous work (Xu et al., 2021) was used, as shown in Figure 1. A sliding window with a pixel size of 224*224 was used to slice the training images into image patches with 50%. The training dataset consisted of 15659 image patches with a pixel size of 224*224. A validation sample set for accuracy evaluation was collected using auxiliary data such as Google Earth optical images and other rice maps. The validation samples were divided into two categories, rice category and non-rice category, and the distribution is shown in Figure 1. Specific information is shown in Table 3.

Table 3 Validation sample set information

Class	Number of plots	Number of pixels
Rice	1913	2,128,431
Non-rice	2032	2,188,477

3.4 U-Net Model

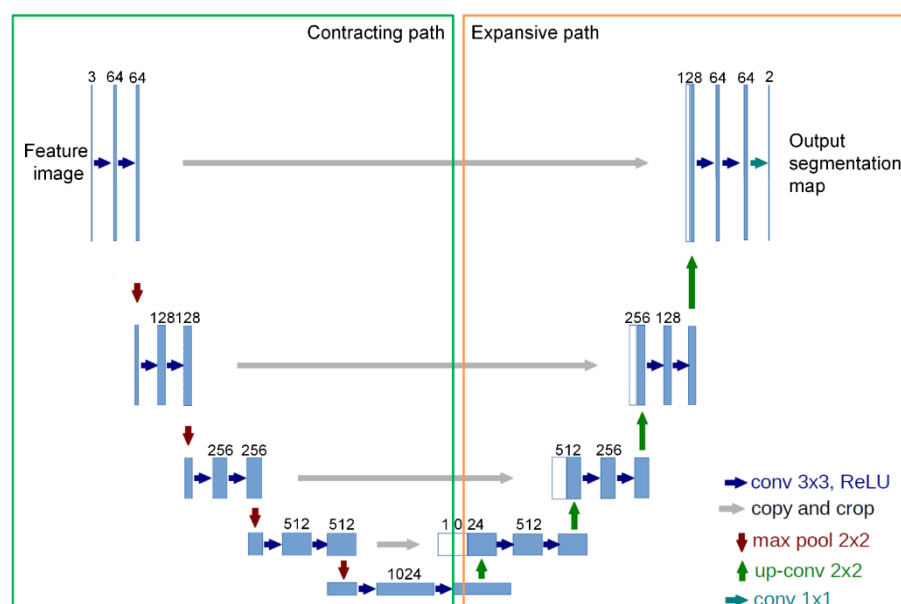
In this paper, high-resolution rice production was accomplished using U-Net. U-Net is a classical semantic segmentation model widely used in biomedical image segmentation and remote sensing (Wei et al., 2019). It outputs semantically labeled



pixel-by-pixel images corresponding to the input image while extracting high-level semantic features, so that the spatial details of the input image can be maintained (Ronneberger et al., 2015).

The structure of U-Net model is shown in Figure 5. The model has 23 convolutional layers, including eighteen 3*3 convolutional layers, four 2*2 convolutional layers and one 1*1 convolutional layer. U-Net consists of encoder (contracting path) and decoder (expansive path). The encoder part consists of five downsampling units, where each unit consists of two 3*3 convolutional layers and a 2*2 max-pool layer. The output of the downsampling unit is input to the next downsampling unit by max-pooling. The decoder contains four upsampling units, each of which consists of two 3*3 convolutional layers and a 2*2 deconvolutional layer. In the final stage of the decoder, the feature vector of the last upsampling units converted into a probability mapping by the 1*1 convolutional layer. The dimension of the probability mapping is 2 and the pixel value indicates the probability that the pixel belongs to rice and non-rice.

To solve the problem of uneven data distribution, a batch normalization (BN) layer was added before each convolutional layer (Ioffe and Szegedy, 2015). The BN layer allows the input data to follow the same distribution to achieve regularization of the model.



270 **Figure 5: Structure of the U-Net model.**

3.5 Postprocessing

In rice mapping, water bodies (e.g., rivers and lakes) can confuse the flooding period signal of rice. In addition, vegetation may cause some disturbances due to weather effects.

Therefore, as drawn on many studies (Lavreniuk et al., 2018; Cué La Rosa et al., 2019; Sun et al., 2021), water body masks and woodland masks produced by WorldCover were used to reduce false alarms of rice extraction results to some extent.



3.6 Accuracy evaluation

In this study, several strategies were used to evaluate our rice map product, including accuracy assessments based on validation sets and comparisons with statistical data and other rice maps at the national and provincial levels. First, common accuracy metrics based on the validation set were calculated to measure the classification effectiveness of the model, including accuracy, precision, recall, and kappa (Congalton, 1991; Vapnik, 1999; Mchugh, 2012).

$$Accuracy = \frac{TP + TN}{TP + TN + FN + FP} \quad (4)$$

$$Precision = \frac{TP}{TP + FP} \quad (5)$$

$$Recall = \frac{TP}{TP + FN} \quad (6)$$

$$Kappa = \frac{accuracy - P_e}{1 - P_e} \quad (7)$$

$$P_e = \frac{(TP + FP) \times (TP + FN) + (FN + TN) \times (FP + TN)}{(TP + TN + FN + FP)^2} \quad (8)$$

where TP denotes the number of pixels correctly classified as rice, TN denotes the number of pixels correctly classified as non-rice, FP denotes the number of pixels misclassified as rice among non-rice pixels, FN denotes the number of pixels misclassified as non-rice among rice pixels, and P_e is the desired accuracy.

Second, the spatial consistency of rice extraction results with statistical data and other rice maps was compared at the national and provincial levels. The coefficient of determination (R^2) of the rice map with statistical data and other rice maps was calculated using the following equation (Draper and Smith, 1998).

$$R^2 = \frac{(\sum_{i=1}^n (x_i - \bar{x}_i) \times (k_i - \bar{k}_i))^2}{\sum_{i=1}^n (x_i - \bar{x}_i)^2 \times \sum_{i=1}^n (k_i - \bar{k}_i)^2} \quad (9)$$

where n is the total number of administrative units, x_i is the area of extracted rice, \bar{x}_i is its corresponding mean value, k_i is the area of statistical data or other rice maps and \bar{k}_i is its corresponding mean value.

4 Results

The 2019 rice map for mainland Southeast Asia using Sentinel-1 SAR data was shown in Figure 6. According to the extraction result, the main rice production areas in Myanmar are located in the Ayeyarwady, Bago and Yangon delta regions, which are crossed by river systems. In addition, Mandalay, Sagaing and Magwayue in the northern arid mountainous region also play an important role in rice production. Thailand's rice fields are concentrated in the central plains, north and northeast. The main rice-producing areas in Laos are located in the central and southern lowland areas. Many of the major rice-producing provinces are located along the Mekong River, such as Bolikhamxai, Khammouan, Savannakhet, Salavan, and Champasak. Rice fields



in Cambodia are concentrated in the Tonle Sap Lake basin and the southern Mekong River basin. The representative rice growing areas in Vietnam are the Mekong Delta and the Red River Delta.

Next, the rice map was evaluated as comprehensive as possible from three different scales. First, the validation sample set introduced in the previous section was used to evaluate the accuracy of rice mapping from the methodological level. Second, at the national level, the rice maps were compared with statistical data on rice harvested area and other available rice maps, respectively. Finally, at the provincial level, more detailed comparisons were made with statistical data and other provincial rice maps to measure the spatial consistency between the extracted rice distribution and these data.

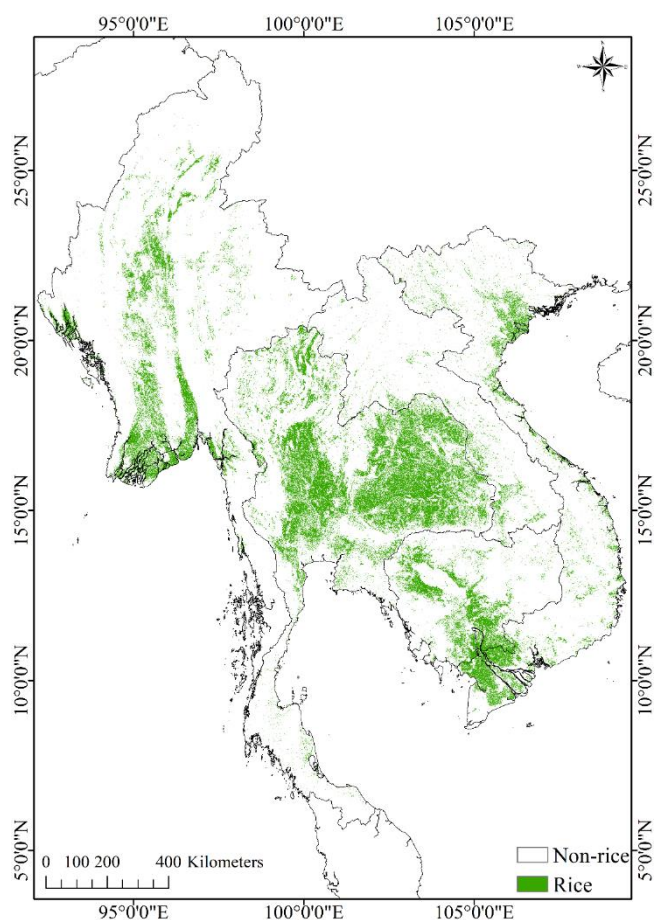


Figure 6: 2019 20m resolution rice map of five countries in mainland Southeast Asia

305 4.1 Accuracy based on the validation set

The accuracies of the rice map based on the validation sample set is shown in Table 4. Among them, the accuracy was as high as 92.20%, and the Kappa was 0.8425, which proved that the proposed method had good classification performance. The precision was 92.45%, which indicated that the method could effectively reduce the false alarms in the rice extraction results.



Therefore, these precision metrics illustrated that the rice mapping results were in good agreement with the validation samples.
 310 It also further demonstrated the capability of the proposed method for rice mapping in large tropical regions.

Table 4 Accuracy of the rice map based on the validation set

Class	Accuracy	Precision	Recall	Kappa
Rice	92.20%	92.45%	90.26%	0.8425

4.2 Comparison with statistical data and other rice maps at the national scale

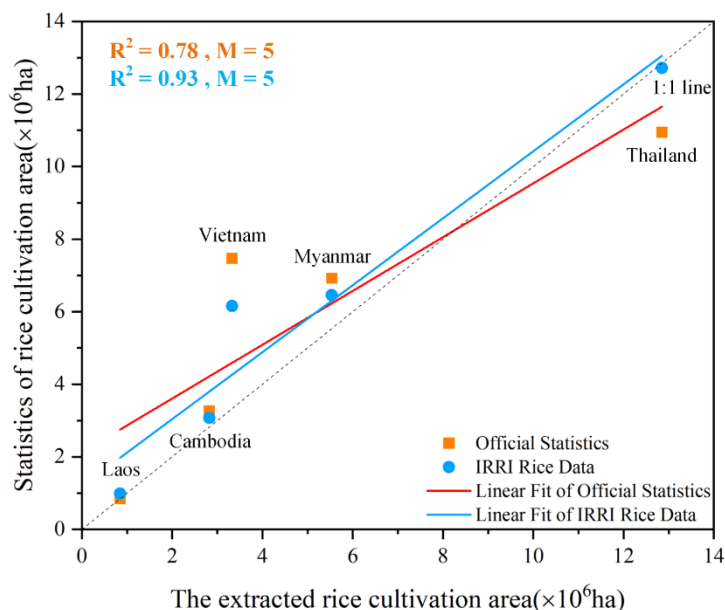
Figure 7 showed the comparison of the extracted rice area with statistical data and the IRRI rice data at the national level scale
 315 for five Southeast Asian countries. As seen from the figure, the extraction results were consistent with both statistical data and
 IRRI rice data. Most points were distributed in the vicinity of the 1:1 line. In contrast, the extraction result was better consistent
 with IRRI, R^2 can reach 0.93, while R^2 with statistical data was 0.78.

Compared with IRRI rice data, the extraction area of Cambodia, Laos and Thailand was close to that of IRRI, while that of
 Myanmar and Vietnam was slight lower. Compared with the statistical data, the extraction areas of Cambodia and Laos were
 320 in good agreement with the statistical data. The extraction area of rice in Myanmar and Vietnam was lower, while that in
 Thailand was slightly higher.

Table 5 showed the statistical area of rice, the area of other rice maps and the area of rice extraction in Vietnam. It could be
 seen that the statistics of rice harvested area were much higher than the area of rice extracted. The statistical data were the total
 rice harvest areas in different growing seasons each year, but the extracted rice area was the land area where rice was planted.
 325 In Vietnam, there are three seasons of rice, namely, spring rice, autumn rice and winter rice, while the harvested areas of spring
 rice and autumn rice are comparable, and the harvested area of winter rice is smaller. In this way, part of the statistical data of
 rice harvest area is repeated and accounts for a large proportion of the area, resulting in a larger rice statistical area than the
 extracted rice area. Although other countries also have multiple rice seasons, the areas of rice in the main season are large,
 while that in other seasons is small, so the area proportion calculated repeatedly is small. The extracted rice area was closer to
 330 the paddy land area in statistical yearbook of Vietnam and VLUCD, indicating that the extraction result was reliable.

Table 5 Statistics, other rice maps and the extracted rice area in Vietnam

Country	Statistics of rice cultivation area (*10 ⁶ ha)	IRRI rice data (*10 ⁶ ha)	Paddy Land area (*10 ⁶ ha)	VLUCD (*10 ⁶ ha)	Extracted rice cultivation area (*10 ⁶ ha)
Vietnam	7.4695	6.1527	4.1205	3.8210	3.3270



335 **Figure 7: Comparison of the extracted rice area with statistical rice harvested area and IIRI dataset at national level scale. M is the number of countries.**

4.3 Comparison with statistical data and other rice maps at the provincial scale

Figure 8 shows the comparison of the extracted rice area with the statistical data of rice harvested area and IIRI rice data at the provincial scale for five Southeast Asian countries. The available rice maps contain a 500 m resolution rice map of mainland
340 Southeast Asia (IIRI Rice Data) and a 30 m resolution rice map of Vietnam (VLUCD) (see Sect. 2.2.3 for details). In general, the rice extraction results were in good agreement with the statistical area, IIRI data and VLUCD. Among them, the R^2 ranged from 0.82 to 0.88 with statistical data and from 0.83 to 0.97 with IIRI, as shown in Figure 8.

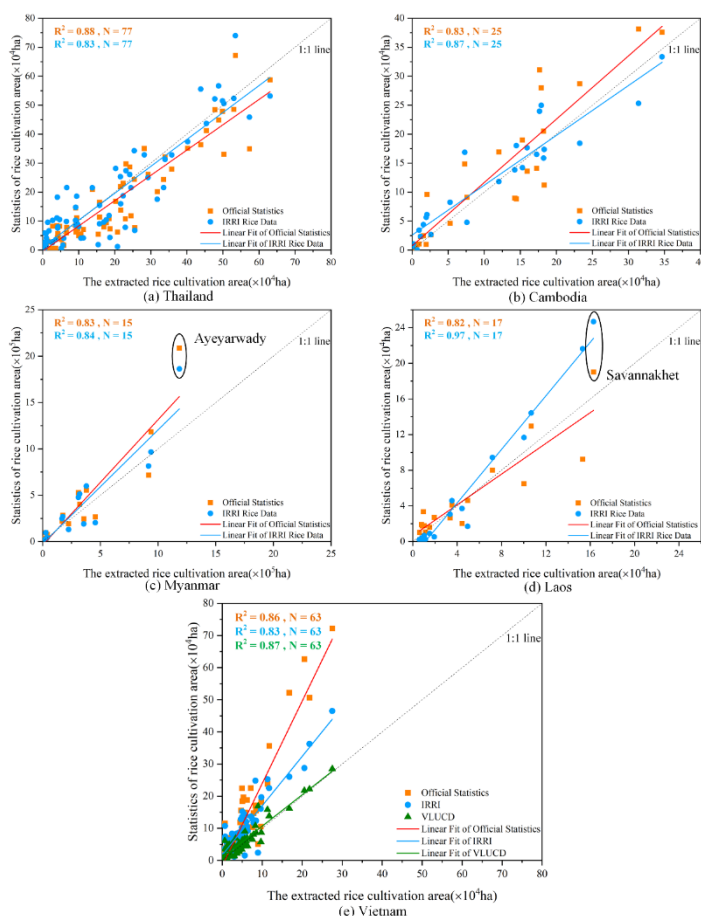
As shown in Figure 8 (a) and (b), the rice planting areas in Thailand and Cambodia extracted by our method had a good correlation with the statistical data and IIRI data at the provincial scale. The R^2 was distributed in the range of 0.83-0.88.
345 There were no provinces with large deviations.

In Figure 8(c), in Myanmar, the R^2 between the extracted area of rice and the statistical data, IIRI rice data was 0.83 and 0.84, respectively. However, the extracted area of Ayeyarwady Province was significantly lower than that of the statistical data and IIRI data. The extraction results of Ayeyarwady were compared with the IIRI data, as shown in Figure 9. As reported by Han et al. (Han et al., 2021), due to the influence of mixed pixels, the IIRI data divides too many rivers and vegetation into rice.
350 And the extracted rice map retains the details of rivers and roads.

The R^2 of the extracted rice area in Laos with statistical data was 0.82, and the highest agreement with IIRI data was 0.97, as shown in Figure 8(d). For the same reason as Ayeyarwady Province, the rice extraction area in Savannakhet Province was lower than the IIRI data because the details of rivers and roads were preserved in the extraction results.



355 Different from other sub figures, Vietnam added data comparison results with 30m VLUCD. The extraction results in Vietnam correlated well with the statistical data, VLUCD and IRRI data, with all R^2 values greater than 0.80, as shown in Figure 8(e). The area of rice extraction in Vietnam was in higher agreement with VLUCD (R^2 of 0.87) than with statistics (R^2 of 0.86) and IRRI Rice Data (R^2 of 0.83). Most of the points of VLUCD were distributed on the 1:1 line.



360 **Figure 8: Comparison of the extracted rice area with statistical rice harvested area and IRRI dataset at provincial scale. N is the number of provinces in each country.**

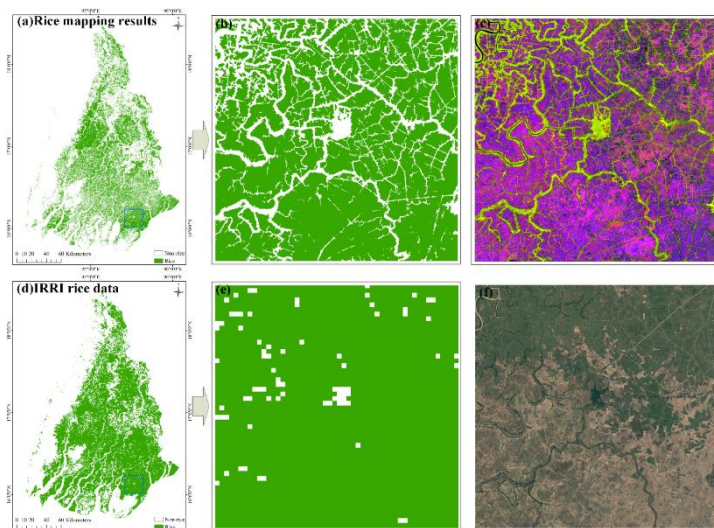


Figure 9: Ayeyarwady's extracted rice area plotted against IRRI data. Our extraction results (a-b), False color image(c), IRRI data (d-e), Google Earth optical image (f) ©Google Earth.

365 5 Discussion

In this study, annual rice maps for five Southeast Asian countries in 2019 were generated using temporal features extracted based on Sentinel-1SAR time series and an improved U-Net. Accuracy, Precision, and Recall based on the validation set exceeded 90% with a Kappa of 0.8425. Accuracy evaluation of rice mapping showed that the proposed temporal features were able to portray the unique growth characteristics of rice, and the improved U-Net model was able to suppress the false alarms of sporadic distribution caused by complex topography. The proposed method has superior capability in mapping rice distribution in large tropical regions.

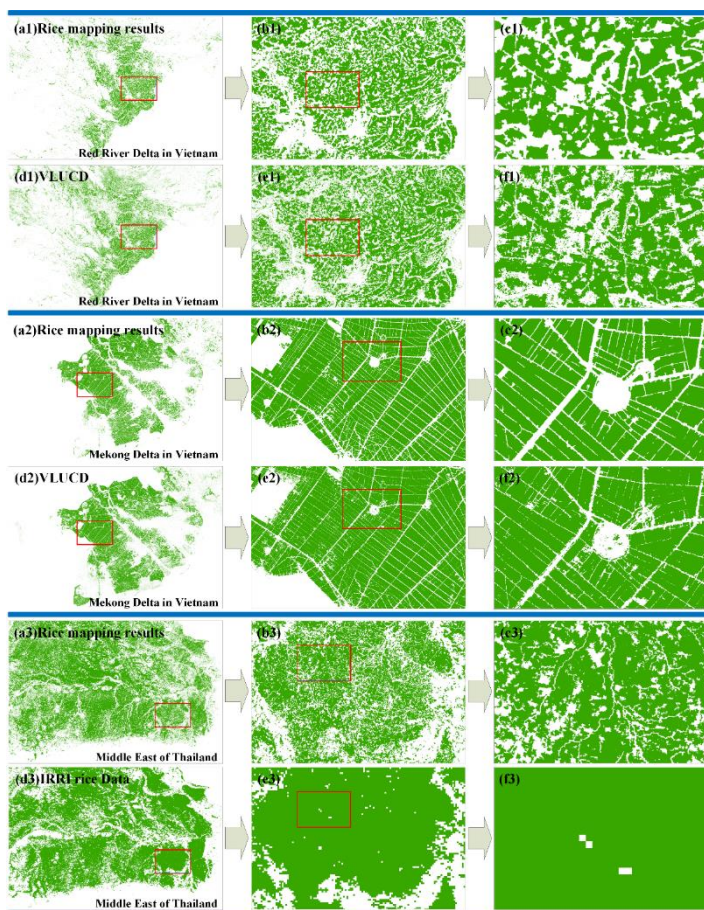
The rice extraction results were compared with statistical data from the national and provincial levels in Sections 4.2 and 4.3. The results of multiple comparisons show that our rice extraction results are in high agreement with the statistical data. However, there were also minor inconsistencies. A possible reason is that the statistical cycle is not strictly aligned with the data collection cycle. The rice area extracted in this study is the total area of all fields that have been planted with rice in a year. Most agricultural statistics record the total area of rice planted in different growing seasons on an annual basis or even from one month of one year to the next. In addition, the statistical methods may cause errors in the statistics. The well-organized rice growing seasons were mainly considered in all statistics, and the random and irregular planting behavior of individual farmers was inevitably ignored. Considering the data collection conditions and statistical errors, it is understandable that the extracted rice maps differ from the official statistics.

The comparison results between rice area products extracted based on different remote sensing data show that our rice extraction results are in good agreement with the available rice products at the national and provincial levels. To fully



385 demonstrate the reliability of the rice extraction results, three subregions from the rice map were selected for comparison in
Thailand and Vietnam, as shown in Figure 10. As mentioned in other literature (Dong et al., 2015; Han et al., 2021), the
MODIS-based IRRI rice map with 500 m resolution contains a large number of mixed image elements, and thus
misclassification exists in the rice results. The spatial distribution characteristics of our rice map were generally consistent
with those of the IRRI data, and our rice map retained more details with fewer mixed pixels. In addition, our rice map also had
better agreement with the spatial distribution and detailed information of rice from VLUCD. Overall, comparisons based on
the validation set, statistical data, and other rice products confirmed the reliability of our generated rice maps.

390 In the study, we found that the temporal features along rivers and wetlands are more similar to rice and have similar colors in
the feature map, which can be easily misclassified as rice. The backscattered information of scattered rice fields is subject to
interference from topography and surrounding non-rice land cover, resulting in missed detection. In future studies, corrections
can be made using water masks extracted from higher precision land cover data.



395

Figure 10 Comparison of our rice maps with available products in typical regions. Our extraction results (a1-c1, a2-c2, a3-c3); VLUCD rice map (d1-f1, d2-f2); IRRI rice Data (d3-f3).



6 Data Availability

The 20 m annual paddy rice map for mainland Southeast Asia can be accessed at Zenodo dataset from the following DOI:
400 <https://doi.org/10.5281/zenodo.7315076>(Sun, 2022). The spatial reference system of the dataset is EPSG:4326(WGS84).

7 Conclusions

Ending hunger and malnutrition in Southeast Asia is essential and rice plays a critical role. Rice is the single most important staple in the region as it provides 50% of calorie intake for its population. Satellite-based remote sensing offers the most practical means of monitoring changes on the vast area of land under rice cultivation in mainland Southeast Asia, given the
405 synoptic coverage, repeated and regular observation, and archival nature of satellite imagery. Questions remain, however, as to appropriate timing, number of satellite observations, spatial resolution of satellite imagery, and effective data processing methods for accurately capturing changes in factors such as rice production extent, growing seasons, and land management. For large-scale rice mapping in tropical and subtropical regions, a rice mapping method based on time series SAR features and deep learning models is proposed. Rice mapping was completed for mainland Southeast Asia using the 2019 Sentinel-1 time
410 series data and the proposed rice extraction method. The accuracy of the proposed method on the validation sample set was 92.20%. Our rice maps correlated significantly with statistical data and were consistent with other rice maps. These results demonstrate the advantages of the proposed method for rice extraction with complex cropping patterns. The rice maps we produced will provide data support for agricultural resource studies, such as yield prediction and agricultural management.

415 **Author Contributions:** Conceptualization, methodology, software, C.S. and H.Z.; validation, formal analysis, H.Z.; investigation, C.S. and L.X.; resources, data curation, J.J. and J.G.; writing—original draft preparation, C.S. and H.Z.; writing—review and editing, H.Z., L.X., J.G. and L.Z.; visualization, L.X. and J.G.; supervision, project administration, H.Z. and C.W. All authors have read and agreed to the published version of the manuscript.

420 **Funding:** This research was funded by the National Natural Science Foundation of China under Grants 41971395, 41930110 and 42001278 and the Strategic Priority Research Program of Chinese Academy of Sciences (XDA19090119).

Acknowledgments: The authors would like to thank ESA and EU Copernicus Program for providing the Sentinel-1 SAR data.

Conflicts of Interest: The authors declare no conflict of interest.

References

425 Bridhikitti, A. and Overcamp, T. J.: Estimation of Southeast Asian rice paddy areas with different ecosystems from moderate-resolution satellite imagery, *Agriculture, Ecosystems & Environment*, 146, 113-120, 2012.
Chang, L., Chen, Y.-T., Chan, Y.-L., and Wu, M.-C.: A Novel Feature for Detection of Rice Field Distribution Using Time Series SAR Data, *IGARSS 2020 - 2020 IEEE International Geoscience and Remote Sensing Symposium*, 10.1109/igarss39084.2020.9323278, 2020.



- 430 Chen, C. F., Son, N. T., and Chang, L. Y.: Monitoring of rice cropping intensity in the upper Mekong Delta, Vietnam using time-series MODIS data, *Advances in Space Research*, 49, 292-301, 10.1016/j.asr.2011.09.011, 2012.
- Chen, C. F., Son, N. T., Chen, C. R., Chang, L. Y., and Chiang, S. H.: Rice Crop Mapping Using Sentinel-1a Phenological Metrics, *ISPRS - International Archives of the Photogrammetry, Remote Sensing and Spatial Information Sciences*, XLI-B8, 863-865, 10.5194/isprsarchives-XLI-B8-863-2016, 2016.
- 435 Clauss, K., Yan, H., and Kuenzer, C.: Mapping Paddy Rice in China in 2002, 2005, 2010 and 2014 with MODIS Time Series, *Remote Sensing*, 8, 10.3390/rs8050434, 2016.
- Clauss, K., Ottinger, M., Leinenkugel, P., and Kuenzer, C.: Estimating rice production in the Mekong Delta, Vietnam, utilizing time series of Sentinel-1 SAR data, *International Journal of Applied Earth Observation and Geoinformation*, 73, 574-585, 10.1016/j.jag.2018.07.022, 2018.
- 440 Congalton, R. G.: A review of assessing the accuracy of classifications of remotely sensed data, *Remote sensing of environment*, 37, 35-46, 1991.
- Crisóstomo de Castro Filho, H., Abílio de Carvalho Júnior, O., Ferreira de Carvalho, O. L., Pozzobon de Bem, P., dos Santos de Moura, R., Olino de Albuquerque, A., Rosa Silva, C., Guimarães Ferreira, P. H., Fontes Guimarães, R., and Trancoso Gomes, R. A.: Rice Crop Detection Using LSTM, Bi-LSTM, and Machine Learning Models from Sentinel-1 Time Series, *Remote Sensing*, 12, 10.3390/rs12162655, 2020.
- 445 Cué La Rosa, L. E., Queiroz Feitosa, R., Nigri Happ, P., Del'Arco Sanches, I., and Ostwald Pedro da Costa, G. A.: Combining Deep Learning and Prior Knowledge for Crop Mapping in Tropical Regions from Multitemporal SAR Image Sequences, *Remote Sensing*, 11, 10.3390/rs11172029, 2019.
- Desa, U.: *Transforming our world: The 2030 agenda for sustainable development*, 2016.
- Dong, J., Xiao, X., Menarguez, M. A., Zhang, G., Qin, Y., Thau, D., Biradar, C., and Moore, B.: 3rd: Mapping paddy rice planting area in northeastern Asia with Landsat 8 images, phenology-based algorithm and Google Earth Engine, *Remote Sens Environ*, 185, 142-154, 10.1016/j.rse.2016.02.016, 2016a.
- 450 Dong, J., Xiao, X., Zhang, G., Menarguez, M., Choi, C., Qin, Y., Luo, P., Zhang, Y., and Moore, B.: Northward expansion of paddy rice in northeastern Asia during 2000–2014, *Geophysical research letters*, 43, 3754-3761, 2016b.
- Dong, J., Xiao, X., Kou, W., Qin, Y., Zhang, G., Li, L., Jin, C., Zhou, Y., Wang, J., Biradar, C., Liu, J., and Moore, B.: Tracking the dynamics of paddy rice planting area in 1986–2010 through time series Landsat images and phenology-based algorithms, *Remote Sensing of Environment*, 160, 99-113, 10.1016/j.rse.2015.01.004, 2015.
- 455 Draper, N. R. and Smith, H.: *Applied regression analysis*, John Wiley & Sons 1998.
- FAO: World rice production (Crops > Items > Rice, paddy): <https://www.fao.org/faostat/en/#data/QCL>, last access: 7/11/2022.
- FAOSTAT: Statistical Database of the Food and Agricultural Organization of the United Nations., 2010.
- 460 Filippini, F.: Sentinel-1 GRD Preprocessing Workflow, 3rd International Electronic Conference on Remote Sensing, 10.3390/ecrs-3-06201, 2019.
- Godfray, H. C., Beddington, J. R., Crute, I. R., Haddad, L., Lawrence, D., Muir, J. F., Pretty, J., Robinson, S., Thomas, S. M., and Toulmin, C.: Food security: the challenge of feeding 9 billion people, *Science*, 327, 812-818, 10.1126/science.1185383, 2010.
- Guan, X., Huang, C., Liu, G., Meng, X., and Liu, Q.: Mapping rice cropping systems in Vietnam using an NDVI-based time-series similarity measurement based on DTW distance, *Remote Sensing*, 8, 19, 2016.
- 465 Gumma, M. K., Nelson, A., Thenkabail, P. S., and Singh, A. N.: Mapping rice areas of South Asia using MODIS multitemporal data, *Journal of applied remote sensing*, 5, 053547, 2011a.
- Gumma, M. K., Gauchan, D., Nelson, A., Pandey, S., and Rala, A.: Temporal changes in rice-growing area and their impact on livelihood over a decade: A case study of Nepal, *Agriculture, Ecosystems & Environment*, 142, 382-392, 10.1016/j.agee.2011.06.010, 2011b.
- 470 Gumma, M. K., Thenkabail, P. S., Maunahan, A., Islam, S., and Nelson, A.: Mapping seasonal rice cropland extent and area in the high cropping intensity environment of Bangladesh using MODIS 500 m data for the year 2010, *ISPRS Journal of Photogrammetry and Remote Sensing*, 91, 98-113, 2014.
- Han, J., Zhang, Z., Luo, Y., Cao, J., Zhang, L., Cheng, F., Zhuang, H., Zhang, J., and Tao, F.: NESEA-Rice10: high-resolution annual paddy rice maps for Northeast and Southeast Asia from 2017 to 2019, *Earth System Science Data*, 13, 5969-5986, 10.5194/essd-13-5969-2021, 2021.
- 475 Han, J., Zhang, Z., Luo, Y., Cao, J., Zhang, L., Zhuang, H., Cheng, F., Zhang, J., and Tao, F.: Annual paddy rice planting area and cropping intensity datasets and their dynamics in the Asian monsoon region from 2000 to 2020, *Agricultural Systems*, 200, 10.1016/j.agsy.2022.103437, 2022.
- Hoang-Phi, P., Nguyen-Kim, T., Nguyen-Van-Anh, V., Lam-Dao, N., Le-Van, T., and Pham-Duy, T.: Rice yield estimation in An Giang province, the Vietnamese Mekong Delta using Sentinel-1 radar remote sensing data, *IOP Conference Series: Earth and Environmental Science*, 012001, 2021.
- 480 Huang, X., Wang, J., Shang, J., Liao, C., and Liu, J.: Application of polarization signature to land cover scattering mechanism analysis and classification using multi-temporal C-band polarimetric RADARSAT-2 imagery, *Remote Sensing of Environment*, 193, 11-28, 2017.
- Inoue, S., Ito, A., and Yonezawa, C.: Mapping Paddy fields in Japan by using a Sentinel-1 SAR time series supplemented by Sentinel-2 images on Google Earth Engine, *Remote Sensing*, 12, 1622, 2020.



- 485 Ioffe, S. and Szegedy, C.: Batch normalization: Accelerating deep network training by reducing internal covariate shift, *International conference on machine learning*, 448-456, Jin, X., Kumar, L., Li, Z., Feng, H., Xu, X., Yang, G., and Wang, J.: A review of data assimilation of remote sensing and crop models, *European Journal of Agronomy*, 92, 141-152, 10.1016/j.eja.2017.11.002, 2018.
- 490 Johnson, D. M. and Mueller, R.: The 2009 cropland data layer, *Photogramm. Eng. Remote Sens.*, 76, 1201-1205, 2010.
- Kang, J., Yang, X., Wang, Z., Huang, C., and Wang, J.: Collaborative Extraction of Paddy Planting Areas with Multi-Source Information Based on Google Earth Engine: A Case Study of Cambodia, *Remote Sensing*, 14, 10.3390/rs14081823, 2022.
- Kuenzer, C. and Knauer, K.: Remote sensing of rice crop areas, *International Journal of Remote Sensing*, 34, 2101-2139, 10.1080/01431161.2012.738946, 2012.
- 495 Laborte, A. G., Gutierrez, M. A., Balanza, J. G., Saito, K., Zwart, S. J., Boschetti, M., Murty, M. V. R., Villano, L., Aunario, J. K., Reinke, R., Koo, J., Hijmans, R. J., and Nelson, A.: RiceAtlas, a spatial database of global rice calendars and production, *Sci Data*, 4, 170074, 10.1038/sdata.2017.74, 2017.
- Lavreniuk, M., Kussul, N., Shelestov, A., Dubovyk, O., and Löw, F.: Object-based postprocessing method for crop classification maps, *IGARSS 2018-2018 IEEE International Geoscience and Remote Sensing Symposium*, 7058-7061,
- 500 Li, H., Fu, D., Huang, C., Su, F., Liu, Q., Liu, G., and Wu, S.: An Approach to High-Resolution Rice Paddy Mapping Using Time-Series Sentinel-1 SAR Data in the Mun River Basin, Thailand, *Remote Sensing*, 12, 10.3390/rs12233959, 2020.
- Liu, C.-a., Chen, Z.-x., Shao, Y., Chen, J.-s., Hasi, T., and Pan, H.-z.: Research advances of SAR remote sensing for agriculture applications: A review, *Journal of Integrative Agriculture*, 18, 506-525, 10.1016/s2095-3119(18)62016-7, 2019.
- Liu, R., Zhang, G., Dong, J., Zhou, Y., You, N., He, Y., and Xiao, X.: Evaluating Effects of Medium-Resolution Optical Data Availability on Phenology-Based Rice Mapping in China, *Remote Sensing*, 14, 10.3390/rs14133134, 2022.
- 505 Liu, Z., Hu, Q., Tan, J., and Zou, J.: Regional scale mapping of fractional rice cropping change using a phenology-based temporal mixture analysis, *International Journal of Remote Sensing*, 40, 2703-2716, 10.1080/01431161.2018.1530812, 2018.
- Luo, Y., Zhang, Z., Chen, Y., Li, Z., and Tao, F.: ChinaCropPhen1km: a high-resolution crop phenological dataset for three staple crops in China during 2000–2015 based on leaf area index (LAI) products, *Earth System Science Data*, 12, 197-214, 2020a.
- Luo, Y., Zhang, Z., Li, Z., Chen, Y., Zhang, L., Cao, J., and Tao, F.: Identifying the spatiotemporal changes of annual harvesting areas for three staple crops in China by integrating multi-data sources, *Environmental Research Letters*, 15, 10.1088/1748-9326/ab80f0, 2020b.
- 510 Manjunath, K., More, R. S., Jain, N., Panigrahy, S., and Parihar, J.: Mapping of rice-cropping pattern and cultural type using remote-sensing and ancillary data: A case study for South and Southeast Asian countries, *International Journal of Remote Sensing*, 36, 6008-6030, 2015.
- Mansaray, L. R., Kabba, V. T. S., Zhang, L., and Bebeley, H. A.: Optimal multi-temporal Sentinel-1A SAR imagery for paddy rice field discrimination; a recommendation for operational mapping initiatives, *Remote Sensing Applications: Society and Environment*, 22, 10.1016/j.rsase.2021.100533, 2021.
- 515 McHugh, M. L.: Interrater reliability: the kappa statistic, *Biochemia medica*, 22, 276-282, 2012.
- Mosleh, M. K., Hassan, Q. K., and Chowdhury, E. H.: Application of remote sensors in mapping rice area and forecasting its production: a review, *Sensors (Basel)*, 15, 769-791, 10.3390/s150100769, 2015.
- 520 Ndikumana, E., Ho Tong Minh, D., Baghdadi, N., Courault, D., and Hossard, L.: Deep Recurrent Neural Network for Agricultural Classification using multitemporal SAR Sentinel-1 for Camargue, France, *Remote Sensing*, 10, 10.3390/rs10081217, 2018.
- Nelson, A. and Gumma, M. K.: A map of lowland rice extent in the major rice growing countries of Asia [dataset], 2015.
- Nelson, A., Setiyono, T., Rala, A., Quicho, E., Raviz, J., Abonete, P., Maunahan, A., Garcia, C., Bhatti, H., Villano, L., Thongbai, P., Holecz, F., Barbieri, M., Collivignarelli, F., Gatti, L., Quilang, E., Mabalay, M., Mabalot, P., Barroga, M., Bacong, A., Detoito, N., Berja, G., Varquez, F., Wahyunto, Kuntjoro, D., Murdiyati, S., Pazhanivelan, S., Kannan, P., Mary, P., Subramanian, E., Rakwatin, P., Intrman, A., Setapayak, T., Lertna, S., Minh, V., Tuan, V., Duong, T., Quyen, N., Van Kham, D., Hin, S., Veasna, T., Yadav, M., Chin, C., and Ninh, N.: Towards an Operational SAR-Based Rice Monitoring System in Asia: Examples from 13 Demonstration Sites across Asia in the RIICE Project, *Remote Sensing*, 6, 10773-10812, 10.3390/rs61110773, 2014.
- 525 Nguyen, D. B. and Wagner, W.: European Rice Cropland Mapping with Sentinel-1 Data: The Mediterranean Region Case Study, *Water*, 9, 10.3390/w9060392, 2017.
- 530 Ni, R., Tian, J., Li, X., Yin, D., Li, J., Gong, H., Zhang, J., Zhu, L., and Wu, D.: An enhanced pixel-based phenological feature for accurate paddy rice mapping with Sentinel-2 imagery in Google Earth Engine, *ISPRS Journal of Photogrammetry and Remote Sensing*, 178, 282-296, 10.1016/j.isprsjprs.2021.06.018, 2021.
- Orynbaikyzy, A., Gessner, U., and Conrad, C.: Crop type classification using a combination of optical and radar remote sensing data: a review, *International Journal of Remote Sensing*, 40, 6553-6595, 10.1080/01431161.2019.1569791, 2019.
- 535 Pan, B., Zheng, Y., Shen, R., Ye, T., Zhao, W., Dong, J., Ma, H., and Yuan, W.: High Resolution Distribution Dataset of Double-Season Paddy Rice in China, *Remote Sensing*, 13, 10.3390/rs13224609, 2021.
- Phan, D. C., Trung, T. H., Truong, V. T., Sasagawa, T., Vu, T. P. T., Bui, D. T., Hayashi, M., Tadono, T., and Nasahara, K. N.: First comprehensive quantification of annual land use/cover from 1990 to 2020 across mainland Vietnam, *Sci Rep*, 11, 9979, 10.1038/s41598-021-89034-5, 2021.



- 540 Qiu, B., Hu, X., Chen, C., Tang, Z., Yang, P., Zhu, X., Yan, C., and Jian, Z.: Maps of cropping patterns in China during 2015-2021, *Sci Data*, 9, 479, 10.1038/s41597-022-01589-8, 2022.
- Ronneberger, O., Fischer, P., and Brox, T.: U-net: Convolutional networks for biomedical image segmentation, *International Conference on Medical image computing and computer-assisted intervention*, 234-241, 2015
- 545 Shew, A. M. and Ghosh, A.: Identifying Dry-Season Rice-Planting Patterns in Bangladesh Using the Landsat Archive, *Remote Sensing*, 11, 10.3390/rs11101235, 2019.
- Singha, M., Dong, J., Zhang, G., and Xiao, X.: High resolution paddy rice maps in cloud-prone Bangladesh and Northeast India using Sentinel-1 data, *Sci Data*, 6, 26, 10.1038/s41597-019-0036-3, 2019.
- Soh, N. C., Shah, R. M., Giap, S. G. E., Setiawan, B. I., and Minasny, B.: High-Resolution Mapping of Paddy Rice Extent and Growth Stages across Peninsular Malaysia Using a Fusion of Sentinel-1 and 2 Time Series Data in Google Earth Engine, *Remote Sensing*, 14, 1875, 2022.
- 550 Sun, C., Zhang, H., Xu, L., Wang, C., and Li, L.: Rice Mapping Using a BiLSTM-Attention Model from Multitemporal Sentinel-1 Data, *Agriculture*, 11, 977, 2021.
- Sun, C., Zhang, H., Ge, J., Wang, C., Li, L., and Xu, L.: Rice Mapping in a Subtropical Hilly Region Based on Sentinel-1 Time Series Feature Analysis and the Dual Branch BiLSTM Model, *Remote Sensing*, 14, 10.3390/rs14133213, 2022.
- 555 Sun, C. Z., Hong, X., Lu, G., Ji, J., Jiang, J., Zuo, L., Lijun, W., Wang, C.: 20 m Annual Paddy Rice Map for Mainland Southeast Asia Using Sentinel-1 SAR Data (1) [dataset], <https://doi.org/10.5281/zenodo.7315076>, 2022.
- Sun, H.-s., Huang, J.-f., Huete, A. R., Peng, D.-l., and Zhang, F.: Mapping paddy rice with multi-date moderate-resolution imaging spectroradiometer (MODIS) data in China, *Journal of Zhejiang University-Science A*, 10, 1509-1522, 2009.
- 560 Thenkabail, P. S., Biradar, C. M., Noojipady, P., Dheeravath, V., Li, Y., Velpuri, M., Gumma, M., Gangalakunta, O. R. P., Turrall, H., and Cai, X.: Global irrigated area map (GIAM), derived from remote sensing, for the end of the last millennium, *International Journal of Remote Sensing*, 30, 3679-3733, 2009.
- Torbick, N., Chowdhury, D., Salas, W., and Qi, J.: Monitoring Rice Agriculture across Myanmar Using Time Series Sentinel-1 Assisted by Landsat-8 and PALSAR-2, *Remote Sensing*, 9, 10.3390/rs9020119, 2017.
- Torres, R., Snoeij, P., Geudtner, D., Bibby, D., Davidson, M., Attema, E., Potin, P., Rommen, B., Floury, N., and Brown, M.: GMES Sentinel-1 mission, *Remote sensing of environment*, 120, 9-24, 2012.
- 565 Tsokas, A., Rysz, M., Pardalos, P. M., and Dipple, K.: SAR data applications in earth observation: An overview, *Expert Systems with Applications*, 205, 10.1016/j.eswa.2022.117342, 2022.
- Vapnik, V. N.: An overview of statistical learning theory, *IEEE transactions on neural networks*, 10, 988-999, 1999.
- Wei, J., Cui, Y., Luo, W., and Luo, Y.: Mapping Paddy Rice Distribution and Cropping Intensity in China from 2014 to 2019 with Landsat Images, Effective Flood Signals, and Google Earth Engine, *Remote Sensing*, 14, 759, 2022.
- 570 Wei, P., Chai, D., Lin, T., Tang, C., Du, M., and Huang, J.: Large-scale rice mapping under different years based on time-series Sentinel-1 images using deep semantic segmentation model, *ISPRS Journal of Photogrammetry and Remote Sensing*, 174, 198-214, 10.1016/j.isprsjprs.2021.02.011, 2021.
- Wei, S., Zhang, H., Wang, C., Wang, Y., and Xu, L.: Multi-Temporal SAR Data Large-Scale Crop Mapping Based on U-Net Model, *Remote Sensing*, 11, 10.3390/rs11010068, 2019.
- 575 Weiss, M., Jacob, F., and Duveiller, G.: Remote sensing for agricultural applications: A meta-review, *Remote Sensing of Environment*, 236, 10.1016/j.rse.2019.111402, 2020.
- Xiao, X., Boles, S., Frolking, S., Li, C., Babu, J. Y., Salas, W., and Moore III, B.: Mapping paddy rice agriculture in South and Southeast Asia using multi-temporal MODIS images, *Remote sensing of Environment*, 100, 95-113, 2006.
- 580 Xiao, X., Boles, S., Liu, J., Zhuang, D., Frolking, S., Li, C., Salas, W., and Moore III, B.: Mapping paddy rice agriculture in southern China using multi-temporal MODIS images, *Remote sensing of environment*, 95, 480-492, 2005.
- Xin, F., Xiao, X., Dong, J., Zhang, G., Zhang, Y., Wu, X., Li, X., Zou, Z., Ma, J., Du, G., Doughty, R. B., Zhao, B., and Li, B.: Large increases of paddy rice area, gross primary production, and grain production in Northeast China during 2000-2017, *Sci Total Environ*, 711, 135183, 10.1016/j.scitotenv.2019.135183, 2020.
- 585 Xu, L., Zhang, H., Wang, C., Wei, S., Zhang, B., Wu, F., and Tang, Y.: Paddy Rice Mapping in Thailand Using Time-Series Sentinel-1 Data and Deep Learning Model, *Remote Sensing*, 13, 3994, 2021.
- Yang, L., Wang, L., Huang, J., Mansaray, L. R., and Mijiti, R.: Monitoring policy-driven crop area adjustments in northeast China using Landsat-8 imagery, *International Journal of Applied Earth Observation and Geoinformation*, 82, 10.1016/j.jag.2019.06.002, 2019.
- 590 Yang, L., Huang, R., Huang, J., Lin, T., Wang, L., Mijiti, R., Wei, P., Tang, C., Shao, J., Li, Q., and Du, X.: Semantic Segmentation Based on Temporal Features: Learning of Temporal-Spatial Information From Time-Series SAR Images for Paddy Rice Mapping, *IEEE Transactions on Geoscience and Remote Sensing*, 1-16, 10.1109/tgrs.2021.3099522, 2021.
- You, N. and Dong, J.: Examining earliest identifiable timing of crops using all available Sentinel 1/2 imagery and Google Earth Engine, *ISPRS Journal of Photogrammetry and Remote Sensing*, 161, 109-123, 10.1016/j.isprsjprs.2020.01.001, 2020.
- 595 You, N., Dong, J., Huang, J., Du, G., Zhang, G., He, Y., Yang, T., Di, Y., and Xiao, X.: The 10-m crop type maps in Northeast China during 2017-2019, *Sci Data*, 8, 41, 10.1038/s41597-021-00827-9, 2021.



- Yu, Q., You, L., Wood-Sichra, U., Ru, Y., Joglekar, A. K. B., Fritz, S., Xiong, W., Lu, M., Wu, W., and Yang, P.: A cultivated planet in 2010 – Part 2: The global gridded agricultural-production maps, *Earth System Science Data*, 12, 3545-3572, 10.5194/essd-12-3545-2020, 2020.
- 600 Yuan, S., Stuart, A. M., Laborte, A. G., Rattalino Edreira, J. I., Dobermann, A., Kien, L. V. N., Thúy, L. T., Paothong, K., Traesang, P., Tint, K. M., San, S. S., Villafuerte, M. Q., Quicho, E. D., Pame, A. R. P., Then, R., Flor, R. J., Thon, N., Agus, F., Agustiani, N., Deng, N., Li, T., and Grassini, P.: Southeast Asia must narrow down the yield gap to continue to be a major rice bowl, *Nature Food*, 3, 217-226, 10.1038/s43016-022-00477-z, 2022.
- Zanaga, D., Van De Kerchove, R., De Keersmaecker, W., Souverijns, N., Brockmann, C., Quast, R., Wevers, J., Grosu, A., Paccini, A., and Vergnaud, S.: *ESA WorldCover 10 m 2020 v100*, 2021.
- 605 Zhang, G., Xiao, X., Biradar, C. M., Dong, J., Qin, Y., Menarguez, M. A., Zhou, Y., Zhang, Y., Jin, C., Wang, J., Doughty, R. B., Ding, M., and Moore, B., 3rd: Spatiotemporal patterns of paddy rice croplands in China and India from 2000 to 2015, *Sci Total Environ*, 579, 82-92, 10.1016/j.scitotenv.2016.10.223, 2017.
- Zhang, X., Wu, B., Ponce-Campos, G., Zhang, M., Chang, S., and Tian, F.: Mapping up-to-Date Paddy Rice Extent at 10 M Resolution in China through the Integration of Optical and Synthetic Aperture Radar Images, *Remote Sensing*, 10, 10.3390/rs10081200, 2018.
- 610 Zhao, R., Li, Y., and Ma, M.: Mapping Paddy Rice with Satellite Remote Sensing: A Review, *Sustainability*, 13, 10.3390/su13020503, 2021.
- Zhu, Z. and Woodcock, C. E.: Object-based cloud and cloud shadow detection in Landsat imagery, *Remote sensing of environment*, 118, 83-94, 2012.